

Measured cross sections and ion energies for a CHF₃ discharge

B. L. Peko^{a)} and R. L. Champion

Department of Physics, College of William and Mary, Williamsburg, Virginia 23187

M. V. V. S. Rao^{b)} and J. K. Olthoff

Electricity Division, Electronics and Electrical Engineering Laboratory, National Institute of Standards and Technology, Gaithersburg, Maryland 20899

(Received 4 March 2002; accepted for publication 10 May 2002)

Trifluoromethane (CHF₃) is used in semiconductor plasma processing chambers to achieve high-etch selectivity of an oxide layer over a silicon substrate. Such surface etching is governed by the ion and molecule fluxes near the surface, the concentrations of which are dependent upon species interactions in and their transport through the plasma. In order to assist in the interpretation of ion flux measurements and to provide fundamental data required for plasma modeling, we report the first total cross sections for significant ion-molecule reactions occurring in CHF₃ discharges. The reactions studied include collision-induced dissociation for CF₃⁺ on CHF₃, dissociative charge transfer for CF₃⁺ and F⁺ on CHF₃, and electron detachment from F⁻ on CHF₃. Collision energies range from a few to a few hundred electron volts. In addition, ion-flux energy distributions and relative ion intensities have been measured and are presented for dc townsend discharges with E/N values ranging from 5×10^{-18} to 25×10^{-18} V m² [5 to 25 kTd]. The townsend discharge results are qualitatively interpreted using the cross-section measurements. © 2002 American Institute of Physics. [DOI: 10.1063/1.1491276]

I. INTRODUCTION

Trifluoromethane is a common feedgas in materials processing applications because it is relatively inert and dissociates readily into chemically reactive ionic and neutral species in a discharge environment. Other positive properties of CHF₃ include its short atmospheric lifetime (250 years)¹ and the fact that high-etch selectivities for SiO₂ over silicon and photoresist can be achieved.²⁻⁷ Because the successful fabrication of microdevices depends on a delicate balance of etching and deposition, it is of paramount importance to understand the physical and chemical interactions that drive these processes. Numerous experiments have been conducted that focus on varying discharge parameters, such as power, pressure, and admixture concentration, in order to optimize etch rate and selectivity.³⁻⁹ In select instances, modeling of the observations is done.¹⁰⁻¹² This is a difficult task because, despite the fact that much work has been done to characterize electron interactions with CHF₃,¹³⁻¹⁴ almost no quantitative information is available concerning ion-molecule interactions that occur in these discharges. Such data are essential because of the important role that secondary products from ion-molecule reactions play in the etching and deposition processes. Owing to this lack of data, plasma models may employ estimates of cross-section values,¹⁰ or in some cases even ignore potentially important ion-molecule reactions.

In the same spirit as our previous work involving CF₄,¹⁵ we add to the minimal amount of ion-molecule interaction data available for plasma processing models by presenting

the results of two distinct experiments. From the first experiment, we present measured absolute cross sections for ion-molecule reactions typically found in CHF₃ discharges. The reactions studied include: dissociative charge transfer (DCT) for collisions of F⁺ and CF₃⁺ with CHF₃, collision-induced dissociation (CID) for CF₃⁺ impacting CHF₃, and collisional electron detachment (ED) for F⁻ on CHF₃. The relative collision energy range investigated is 20–400 eV, which is comparable to ion energies found in discharge environments. From the second experiment, we present relative ion-flux intensities and kinetic-energy distributions for ions generated in dc townsend discharges in CHF₃. The electric field-to-gas density ratio, E/N, range for these discharges is 5×10^{-18} – 25×10^{-18} V m² [5–25 kTd]. The ion data from the townsend discharge experiments are used as an example of how discharge data can be more fully interpreted in light of the cross-section measurements.

II. EXPERIMENTAL METHODS

The experimental arrangements and operating conditions employed for the cross-section and ion-flux measurements are identical to those used in our study of CF₄ discharges.¹⁵⁻¹⁷ Only a brief description of each experiment will be provided here.

For the cross-section experiments, complementary electrostatic trapping cell and crossed-beam techniques were used. The primary ions were formed in a low-pressure (~1.3 Pa) arc discharge source with the source gas comprised of a 9:1, Ar:CF₄ mixture. After extraction and mass analysis the primary ions were focused into an electrostatic trapping cell for the measurement of total cross sections for CID, ED, or the summed cross section for all DCT reaction channels. For

^{a)}Present address: Department of Physics and Astronomy, University of Denver, Denver, CO 80208-2238; electronic mail: bpeko@du.edu

^{b)}Present address: NASA/Ames Research Center, Moffet Field, CA 94035-1000.

the electron detachment cross sections, the free electrons produced were uniquely detected by isolating and confining them to a small radius of gyration with an axial magnetic field. This same scheme was used to measure the target ionization cross section for the F^+ and CF_3^+ primaries, which was found to be negligible ($\leq 0.01 \text{ \AA}^2$) for both primary ions. In order to determine the cross sections for each individual DCT reaction channel the primary ions were intersected orthogonally with a beam of CHF_3 . Product ions with minimal kinetic energy were extracted, mass analyzed, and subsequently counted. From these values, branching ratios were calculated. The relative branching ratios were then combined with the total absolute DCT cross sections found with the trapping cell to determine the cross section for each DCT reaction channel. The collision-induced dissociation and electron detachment cross-section measurements have uncertainties of $\pm 15\%$ while uncertainties for dissociative charge-transfer measurements are $\pm 25\%$.

For the Townsend discharge experiments, the ion-flux energy distributions and relative ion intensities were measured in a parallel plate discharge cell which has been described in detail elsewhere.^{15,18,19} Pressures for these discharges in CHF_3 ranged from approximately 5 to 20 Pa with discharge currents kept below $\sim 100 \mu\text{A}$ to minimize space-charge effects. Ions formed in the discharge were extracted through a 0.1 mm hole in the cathode and subsequently energy and mass analyzed.¹⁸ This apparatus can detect positive and negative ions, however F^- was the only negative ion observed, exhibiting a weak signal compared to the positive ions. The ion-flux energy distributions presented here were derived^{18,19} from the kinetic-energy distributions which were determined by setting the quadrupole mass analyzer to transmit ions of a certain mass and then scanning the potential of the analyzer. The relative ion intensities of the ion fluxes were determined by integrating the ion-flux energy distributions for each ion at each E/N . Uncertainties for the ion-flux energy distributions and relative ion intensities presented here are estimated to be $\pm 3\%$.

III. RESULTS AND DISCUSSION

A. Cross sections

1. $F^+ + CHF_3$

Presented in Fig. 1 are dissociative charge-transfer cross sections plotted as a function of relative collision energy for F^+ on CHF_3 . Two points clearly illustrated in Fig. 1 are the CF^+ is the ion most likely to be produced from dissociative charge transfer for F^+ impinging on CHF_3 , and that the summed cross section for F^+ destruction is large, $\sim 23 \text{ \AA}^2$ on average for the energy range studied. For clarity, the cross sections for some product ions have been omitted from Fig. 1. A complete list of all DCT reaction pathways, as well as all reaction channels studied here is given in Table I. The cross sections for the DCT channels not presented in Fig. 1 (Reactions 1, 4–6, 8, 10) each are less than 2 \AA^2 and approximately independent of collision energy. Even though the production of CF^+ is quite endothermic ($\sim 3.4 \text{ eV}$), the cross section exceeds that of the competing thermoneutral channel yielding CF_2^+ by a factor of three over the entire

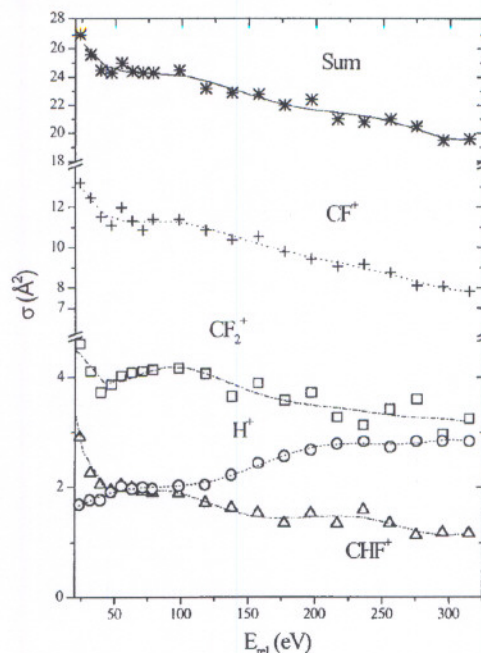


FIG. 1. Dissociative charge-transfer cross sections for $F^+ + CHF_3$ presented as a function of relative collision energy. The summed cross section for reactions 1–10 in Table I is also presented.

energy range studied. In fact, the competing channels for dissociative charge transfer yielding CF_3^+ or CHF_2^+ (Reactions 1 and 6, respectively) are exothermic, and have very small cross sections; such has been observed before for exothermic dissociative charge transfer for F^+/CF_4 system at similar collision energies.¹⁵ In the previous studies of CF_4 , however, CF_2^+ rather than CF^+ was the dominant ion produced. Also, the cross section for CF_2^+ production (Reaction 10) is 0.5 \AA^2 here compared to roughly 5 \AA^2 for the CF_4 target; both processes are endothermic by $\sim 21 \text{ eV}$. Clearly, there is much that remains to be understood regarding these reactions. Finally, in Fig. 1, proton production increases slightly as CHF^+ production decreases suggesting CHF^+ is produced as an excited molecular ion that may further dissociate into H^+ and CF . The energetic threshold for this second dissociation is $\sim 17.2 \text{ eV}$.

2. $CF_3^+ + CHF_3$

Measured DCT cross sections for $CF_3^+ + CHF_3$ are shown in Fig. 2. The product ions CHF_2^+ and CF^+ are most probable. Energetically, Reaction 11 is most favorable, however, the cross section for producing CF_3^+ is small. The cross sections for producing all the other ions (Reactions 12, 14, 16, and 17) are also negligible ($\leq 0.5 \text{ \AA}^2$) over the energy range studied and are not shown. Unlike the results for the F^+ projectile, no H^+ , F^+ , or doubly charged ions were observed. The summed cross section is also considerably less than that for the F^+ projectile and increases sharply as a function of collision energy. This behavior is similar to the CF_4 results.¹⁵

Cross sections were measured for collision-induced dissociation (CID) for these reactants (Reactions 8–21). They were all found to have the same energy-independent magni-

TABLE I. Reaction channels relevant to this work and their ground-state energetics are listed. The majority of the products follow from dissociative charge transfer. The products arising from collision-induced dissociation of CF_3^+ are indicated in curly brackets.

Reaction Number	Reactants	Products	Endothermicity ^a (eV)
1	$F^+ + CHF_3$	$F + CF_3^+ + H$	+2.7
2		$F + CF_2^+ + HF$	-0.2
3		$F + CF^+ + HF + F$	-3.4
4		$F + C^+F_2 + HF$	-15.0
5		$F + CHF_2^+ + F^+$	-13.0
6		$F + CHF_2^+ + F$	+1.1
7		$F + CHF^+ + F_2$	-2.4
8		$F + CH^+ + F_2 + F$	-16.6
9		$F + H^+ + CF_3$	-1.9
10		$F^- + CF_2^+ + HF$	-22.5
11	$CF_3^+ + CHF_3$	$CF_3 + CF_3^+ + H$	-6.2
12		$CF_3 + CF_2^+ + HF$	-8.6
13		$CF_3 + CF^+ + HF + F$	-11.9
14		$CF_3 + C^+ + F_2 + HF$	-18.0
15		$CF_3 + CHF_2^+ + F$	-7.8
16		$CF_3 + CHF^+ + F_2$	-10.8
17		$CF_3 + CH^+ + F_2 + F$	-24.5
18		$\{CF_2^+ + F\} + CHF_3$	-6.2
19		$\{CF^+ + F_2\} + CHF_3$	-7.4
20		$\{F^+ + CF_2\} + CHF_3$	-12.3
21		$\{C^+ + F + F_2\} + CHF_3$	-15.1
22	$F^- + CHF_3$	$F + CHF_3 + e$	-3.4

^aEndothermicities listed were determined from data in Ref. 14 and references cited therein. Positive values indicate an exothermic reaction.

tude, viz. $\sim 6 \text{ \AA}^2$ for $20 < E_{rel} < 225 \text{ eV}$, and are not shown here. The CID channels producing C^+ and F^+ could not be distinguished with the current experimental arrangement¹⁵ due to the similar ion mass. Thus, the summed cross-section values for Reactions 20 and 21 is determined to be $\sim 6 \text{ \AA}^2$. There was no evidence for the production of free electrons which would accompany ionization.

3. $F^- + CHF_3$

Electron detachment cross sections for $F^- + CHF_3$, presented in Fig. 3 as a function of relative collision energy, start at the electron affinity of F and increase rapidly with collision energy. This agrees qualitatively with similar measurements for F^- striking CF_4 (Ref. 15) and rare gas targets.²⁰ These results indicate that electron detachment may be a significant contributor to the neutral fluorine population in a CHF_3 etching discharge.

B. Townsend discharge experiments

The mass spectrum for positive ions striking the cathode of a CHF_3 discharge at $7.5 \times 10^{-18} \text{ V m}^2$ is compared in Fig. 4(a) to that produced by 70 eV electrons colliding with CHF_3 .^{13,14} Again, the only negative ion observed for all E/N values was F^- which exhibited a weak signal intensity, near the threshold sensitivity for the apparatus. Because the actual electron energy distributions for townsend discharges in CHF_3 at these E/N values are unknown, it is an oversimplification to assume that the electron-impact mass spectrum is indicative of the relative distribution of positive ions formed

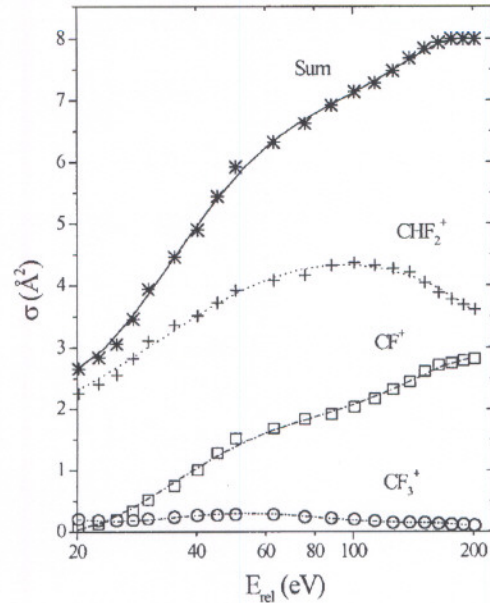


FIG. 2. Absolute cross sections for select DCT channels for the $CF_3^+ + CHF_3$ system. The total cross section for all DCT processes for these reactants is also presented.

in the discharge. It is reasonable to assume, however, that the differences between the two mass spectra are partially attributable to ion-converting collisions experienced by ions as they traverse the discharge. Interestingly, unlike the CF_4 , no doubly charged ions are observed in either mass spectrum.

Clearly missing in Fig. 4(a) is the presence of F^+ in the discharge, it was not observed for any E/N investigated here. This is directly attributable to the large ($\geq 20 \text{ \AA}^2$) DCT cross sections for $F^+ + CHF_3$ (Reactions 1–10) that remove F^+ ions as they traverse the discharge. Additionally, the total cross section for the formation of F^+ ions by DCT (Reaction 5) is small ($\leq 1 \text{ \AA}^2$), and the cross sections for converting CF_3^+ to F^+ and/or C^+ via CID (Reaction 20) are also rela-

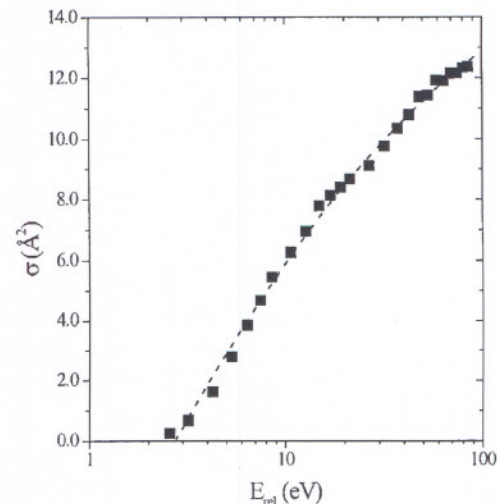


FIG. 3. Electron detachment cross sections for collisions of F^- and CHF_3 .

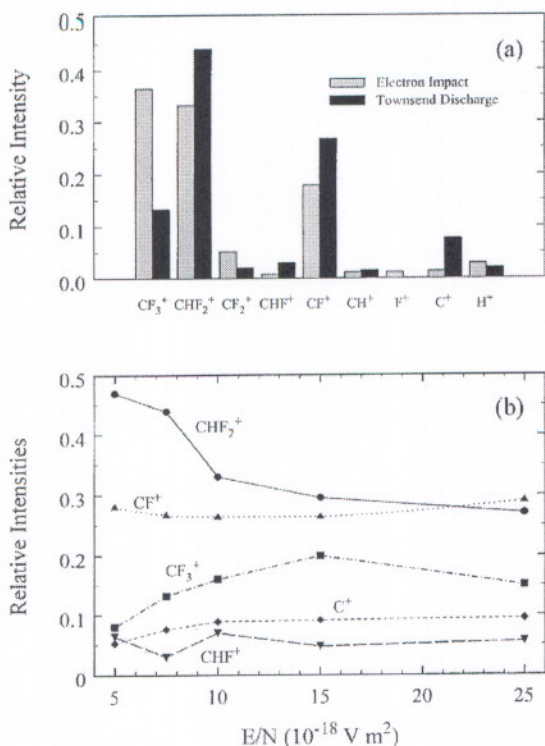


FIG. 4. (a) Comparison of standard electron-impact mass spectrum for CHF_3 for 70 eV electrons, with the mass spectrum of positive ions samples from a CHF_3 townsend discharge with $E/N=7.5 \times 10^{-18} \text{ V m}^{-2}$. The two mass spectra are normalized to have equal total signals. (b) The relative intensities of the five dominant ions sampled from CHF_3 townsend discharges as a function of E/N .

tively small, viz. 6 \AA^2 . Thus, the net effect of ion-molecule collisions in CHF_3 results in a reduction in F^+ ion flux. This is similar to that observed previously for CF_4 .¹⁵

Comparing the mass spectra in Fig. 4(a) also suggests that collisional processes exist that destroy CF_3^+ in a CHF_3 discharge. This observation is supported by the cross-section measurements presented in Sec. III A 2. Specifically, the summed cross section for collision-induced dissociation of CF_3^+ is $\sim 18 \text{ \AA}^2$ (Reactions 18–21), and the summed DCT cross section for $CF_3^+ + CHF_3$ is $\sim 8 \text{ \AA}^2$ at the highest-collision energies (Fig. 2 and Reactions 12–17). Only two reaction channels studied here (Reactions 1 and 11) result in a formed CF_3^+ , and their combined cross section is less than $\sim 1.5 \text{ \AA}^2$.

Two other species that can be surmised to be destroyed by ongoing ion-molecule reactions in the discharge are CF_2^+ and H^+ . The cross sections for producing H^+ are nonzero, $\sim 2.5 \text{ \AA}^2$, thereby suggesting a potential increase in H^+ flux in the discharge. However, protons are highly reactive in discharge environments, and collisional interactions that would deplete free protons are expected to exist. The summed cross section for CF_2^+ production (Reaction 2+12+18) is greater than $\sim 10 \text{ \AA}^2$, one of the largest measured for a particular species. A plausible explanation as to why a corresponding increase in CF_2^+ flux is not observed in the townsend discharge is that CF_2^+ further dissociates via CID

or is converted into other ions as the result of dissociative charge transfer with CHF_3 . Cross sections for these processes remain to be determined.

Conversely, Fig. 4(a) suggests that collisional processes exist which lead to the formation of CHF_2^+ , CHF^+ , CF^+ , and C^+ . This is in agreement with the cross section data shown in Figs. 1 and 2, where all but C^+ have cross sections greater than 2 \AA^2 resulting in their formation. The summed cross section for producing CF^+ from DCT and CID approaches 20 \AA^2 . For many discharge environments CF^+ concentration is observed to be high.^{8,22–24} The cross section for C^+ production from DCT exclusively is $\sim 1 \text{ \AA}^2$, but is production from CID of CF_3^+ (reaction 20+21) has an upper limit of $\sim 6 \text{ \AA}^2$.

The observed relative ion intensities in the townsend discharge, as a function of E/N , can also be discussed in terms of the measured ion-molecule cross sections. In Fig. 4(b), the CF^+ flux is independent of E/N corresponding well to the energy-independent CID and combined DCT cross sections for its production (Figs. 1 and 2). The same can be said for the relatively constant abundance of C^+ ions for $10 \times 10^{-18} \text{ V m}^{-2} \leq E/N \leq 10^{-18} \text{ V m}^{-2}$. The slight decrease in C^+ intensity at lower E/N is most likely due to an anticipated reduction in the relevant CID cross section (Reaction 21) at energies below 20 eV as it approaches its energetic threshold. The fact that CHF_2^+ is the dominant ion observed for nearly all E/N suggests the cross section for the destruction of this ion, once formed, is relatively small and that other pathways may exist that produce this ion. The decrease in CHF_2^+ flux with increasing E/N is consistent with decreasing production of CHF_2^+ above 100 eV (see Fig. 2), and may suggest increasing destruction mechanisms with increasing collision energies. Additional collisional studies involving CHF_2^+ would be useful. The qualitative behavior of the CF_3^+ flux as a function of E/N is difficult to explain because the production cross sections measured here are nearly constant as a function of collisional energy. The decrease of the CF_3^+ population with decreasing E/N suggests that CF_3^+ is readily converted or neutralized at low-collision energies and/or that CF_3^+ production decreases at lower-collision energies. Dissociative ionization of CHF_3 to $CF_3^+ + H$ is exothermic by more than 15 eV and the summed cross section for the production of CF_3^+ from DCT (Reactions 1 and 11) is 2 \AA^2 for all relative collision energies. Furthermore, the summed cross section for the destruction of CF_3^+ via DCT (Reactions 11–17) decreases steadily as the relative energy is decreased, and CID cross sections are expected to decrease for $E_{rel} < 20 \text{ eV}$.

Ion-flux energy distributions for the four most abundant ions in the townsend discharge are presented in Fig. 5 for the two E/N limits investigated here. All ion energy distributions exhibit a linear decay with increasing ion energy on the $5 \times 10^{-18} \text{ V m}^{-2}$ semilog plots. This behavior indicates that the ions are in equilibrium, i.e., each ion undergoes many collisions before striking the cathode.^{18,19} Similar conditions exist for CHF_2^+ and CF_3^+ at $25 \times 10^{-18} \text{ V m}^{-2}$, but CF^+ and C^+ exhibit nonlinear dependencies indicative of nonequilibrium conditions. This suggests that few ion molecule collisions exist for these lighter molecules that result in significant energy loss or destruction.

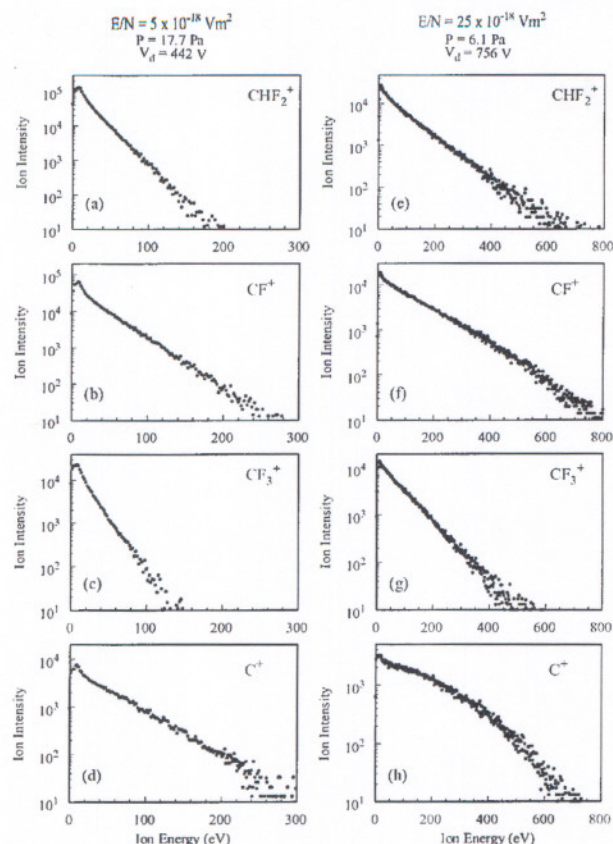


FIG. 5. Ion-flux energy distributions for positive ions sampled from CHF_3 Townsend discharges with $E/N = 5 \times 10^{-18} \text{ V m}^{-2}$ and $25 \times 10^{-18} \text{ V m}^{-2}$.

The corresponding mean energies (not presented) and the maximum ion energy for the distributions, with the exception of H^+ , increase with decreasing mass suggesting that the magnitude of the collisional cross sections for ion energy loss is smaller for less massive ions. The mean energies range from 10 to 70 eV for $E/N = 5$ and 25 kTd , respectively, for CF_3^+ and 50–160 eV for C^+ . The low CF_3^+ ion energy correlates well with the large cross section ($\sim 18 \text{ \AA}^2$) for the destruction of “high” energy CF_3^+ due to CID and its conversion cross section ($\sim 8 \text{ \AA}^2$) from “high”-to-“low” energy via DCT (Reactions 11–17). One can then infer that the cross sections may be similar for CF_2^+ , CHF_2^+ , CF^+ , and C^+ , but somehow scaled according to ion mass.

These observations are consistent with those observed previously for CF_4 ,¹⁵ except that in the previous study, the energy distributions for all the positive and negative ions indicated a lack of equilibrium at high E/N ($\sim 25 \times 10^{-18} \text{ V m}^{-2}$). Only the lightest ions exhibit such behavior in CHF_3 . This is inconsistent with the somewhat larger DCT cross sections measured for CHF_3 as compared to CF_4 .

Intensities of F^- flux were too small to provide reliable ion energy distributions. The relatively small F^- signal is supported by the large cross section for collisional electron detachment (Reaction 22) and the fact that dissociative electron attachment to CHF_3 is improbable.^{13,14}

In addition to the simple dc discharge discussed here, the current cross-section measurements support observations made in more complex plasmas. For example, Haverlag and coworkers¹⁰ report that CF_x radical densities are larger near the electrodes of a capacitively coupled CHF_3 plasma than in the glow region. They suggest that this density gradient is due to inelastic ion-molecule collisions—not surface recombination or sputtering—occurring in the plasma, with cross sections for dissociative charge-transfer and collision-induced dissociation reactions, among others, ranging from 0.1 to 100 \AA^2 . Snijkers *et al.*¹¹ have reported that these same types of reactions occur in rf capacitively coupled CF_4 discharges. The cross sections here support Haverlag’s analysis. The total cross section for the production of CF_3 via the ion-molecule reactions measured here (Reactions 9 and 11–17) is on the order of 14 \AA^2 for $E_{\text{rel}} \geq 100 \text{ eV}$. The only reaction studied here that would produce a CF_2 radical is CID (Reaction 20) for which the cross section is $\sim 6 \text{ \AA}^2$. There are many possible reactions that could produce CF_2^+ which were not studied here, e.g., the neutralization of CF_2^+ from dissociative charge transfer, for which a substantial cross section has been proposed elsewhere in this article. No ion-molecule reactions investigated here produced CF , although these may exist even though no information is currently available for such cross sections.

The mass distributions of positive ions generated in inductively coupled plasmas and other discharges are typically similar to those for electron impact ionization of the feed gas.²¹ There are however examples where this is not the case. In agreement with most observations for CHF_3 plasmas, Kirsme *et al.*⁸ found that for a high-power, low-pressure (1000 W, 1 mTorr) electron cyclotron resonance discharge in CHF_3 that CF^+ was the dominant ion, while the concentration of F^+ is “small.” This is consistent with the Townsend discharges studied here where no F^+ was detected and the CF^+ flux was comparable to CHF_2^+ at high E/N . This suggests that the cross sections for the destruction of F^+ and the formation of CF^+ are of similar importance in these two very different CHF_3 discharges.

In the inductively coupled plasma (ICP) of Wang *et al.*,²¹ it was recently reported that the relative intensities for ions produced via direct ionization all exhibited similar intensities, save for CF_2^+ . This result is quite different from electron impact mass spectra for CHF_3 .^{13,14} In the ICP experiment, the relative CF^+ concentration exceeds that resulting from electron impact of CHF_3 . This can partially be explained by the large cross-section values for CF^+ production measured here (Reactions 3, 13, and 19). Also observed by Wang *et al.* was a relatively high concentration of CF_2^+ and C^+ . The summed cross section for CF_2^+ production (Reactions 2, 12, and 18) is $\sim 10 \text{ \AA}^2$. However, based on the current observations, it appears that the destruction cross section for CF_2^+ must exceed that for its production, namely, 10 \AA^2 . The processes that lead to the destruction of CF_2^+ , DCT, and CID perhaps, would therefore not be considered important in the analysis of the ICP reactor of Wang *et al.* The summed cross section for C^+ production (Reactions 4, 14, and 21) is $\sim 6 \text{ \AA}^2$ and thus it is reasonable to assume that additional reaction pathways play a role in this particular discharge.

CONCLUSIONS

Measured cross sections for ion-molecule reactions occurring in CHF₃ discharges have been presented. A myriad of ions and neutrals are formed from the reactants studied here and a few general conclusions may be drawn. The large cross section for electron detachment $\sim 14 \text{ \AA}^2$, dissociative charge transfer for ionized fluorine $\sim 25 \text{ \AA}^2$, and collision induced dissociation $\sim 6 \text{ \AA}^2$, at large collision energies indicates that neutral fluorine, one of the most important radicals in semiconductor etching, may be a dominant species in discharge environments. The cross section for the production of the CF₃ radical is substantial as well, $\sim 26 \text{ \AA}^2$, for higher-collision energies. For the ions, CF⁺ has the highest-production probability for the collision energies studied followed by CF₂⁺ and CHF₂⁺.

These ion-molecule cross sections have been used to interpret the characteristics of ion kinetic-energy distributions and relative ion intensities measured for dc townsend discharges. It is clear from the analysis that while the reactants chosen for this investigation are important in a CHF₃ plasma, more cross-section measurements of this type are needed to fully assess ion production and transport mechanisms that characterize this simple CHF₃ discharge. In particular, these include collision-induced dissociation and dissociative charge transfer for the ionic species CF₂⁺, CHF₂⁺, CF⁺, and CHF⁺ along with dissociative charge transfer for C⁺.

ACKNOWLEDGMENTS

The work at W&M was supported by the Division of Chemical Sciences, Office of Basic Energy Sciences, U.S. Department of Energy.

¹The 1994 Report of the Scientific Assessment Working Group of IPCC Intergovernmental Panel on Climate Change (unpublished), p. 28.

- ²R. A. Heinecke, *Solid-State Electron.* **18**, 1146 (1975).
- ³N. R. Rueger, M. F. Doemling, M. Schaepekens, J. J. Beulens, T. E. F. M. Standaert, and G. S. Oehrlein, *J. Vac. Sci. Technol. A* **17**, 2492 (1999).
- ⁴G. S. Oehrlein, Y. Zhang, D. Vender, and M. Haverlag, *J. Vac. Sci. Technol. A* **12**, 323 (1994).
- ⁵G. S. Oehrlein, Y. Zhang, D. Vender, and O. Joubert, *J. Vac. Sci. Technol. A* **12**, 333 (1994).
- ⁶M. V. Bazylenko and M. Gross, *J. Vac. Sci. Technol. A* **14**, 2994 (1996).
- ⁷B. Kim, K.-H. Kwon, and S.-H. Park, *J. Vac. Sci. Technol. A* **17**, 2593 (1999).
- ⁸K. H. R. Kirmse, A. E. Wendt, G. S. Oehrlein, and Y. Zhang, *J. Vac. Sci. Technol. A* **12**, 1287 (1994).
- ⁹X. Li, M. Schaepekens, G. S. Oehrlein, R. Ellefson, L. C. Frees, N. Mueller, and N. Korner, *J. Vac. Sci. Technol. A* **17**, 2438 (1999).
- ¹⁰M. Haverlag, W. W. Stoffels, E. Stoffels, G. M. W. Kroesen, and F. J. de Hoog, *J. Vac. Sci. Technol. A* **14**, 384 (1996).
- ¹¹R. J. M. M. Snijders, M. J. M. van Sambeck, M. B. Hoppenbrouwers, G. M. W. Kroesen, and F. J. de Hoog, *J. Appl. Phys.* **79**, 8982 (1996).
- ¹²M. Haverlag, E. Stoffels, G. M. W. Kroesen, and F. J. de Hoog, *J. Vac. Sci. Technol. A* **12**, 3102 (1994).
- ¹³L. G. Christophorou and J. K. Olthoff, *J. Phys. Chem. Ref. Data* **28**, 967 (1999) and references cited therein.
- ¹⁴L. G. Christophorou, J. K. Olthoff, and M. V. V. S. Rao, *J. Phys. Chem. Ref. Data* **26**, 1 (1997).
- ¹⁵B. L. Peko, I. V. Dyakov, R. L. Champion, M. V. V. S. Rao, and J. K. Olthoff, *Phys. Rev. E* **60**, 7449 (1999).
- ¹⁶B. L. Peko, R. L. Champion, and Y. Wang, *J. Chem. Phys.* **104**, 6149 (1996).
- ¹⁷B. L. Peko and R. L. Champion, *J. Chem. Phys.* **107**, 1156 (1997).
- ¹⁸M. V. V. S. Rao, R. J. Van Brunt, and J. K. Olthoff, *Phys. Rev. E* **54**, 5641 (1996).
- ¹⁹M. V. V. S. Rao, R. J. Van Brunt, and J. K. Olthoff, *Phys. Rev. E* **59**, 4565 (1999).
- ²⁰M. S. Huq, L. D. Doverspike, R. L. Champion, and V. A. Esaulov, *J. Phys. B* **15**, 951 (1982).
- ²¹Y. Wang, M. Misakian, A. N. Goyette, and J. K. Olthoff, *J. Appl. Phys.* **88**, 5612 (2000).
- ²²R. Jayaraman, R. T. McGrath, and G. A. Hebner, *J. Vac. Sci. Technol. A* **17**, 1545 (1999).
- ²³M. Schaepekens, N. R. Rueger, J. J. Beulens, X. Li, T. E. F. M. Standaert, P. J. Matsuo, and G. S. Oehrlein, *J. Vac. Sci. Technol. A* **17**, 3272 (1999).
- ²⁴J. K. Olthoff and Y. Wang, *J. Vac. Sci. Technol. A* **17**, 1552 (1999).